2019

Effects of PAG1 on Src-family kinase trafficking in neuroblastoma cells

Makenzie E. Mayfield
University of Montana, Missoula, mm254077@umconnect.umt.edu

Effects of PAG1 on Src-family kinase trafficking in neuroblastoma cells

Makenzie Mayfield
University of Montana
May, 2019

Effect of PAG1 on Src-family kinase trafficking in neuroblastoma cells

Introduction

During embryonic development, a population of multipotent stem cells, known as the neural crest, migrates throughout the body and differentiates into a wide variety of tissues, including melanocytes, peripheral nervous tissue, and craniofacial cartilage. Extracellular cues, secreted by neighboring cells guide neural crest cells towards the correct cell fate, by binding cell-surface receptors to activate intracellular signaling cascades (1).

Neuroblastoma (NB) is a childhood cancer which develops when neural crest cells fail to differentiate and instead continue to proliferate. Neuroblastoma accounts for approximately 8% of pediatric cancers and nearly 15% of cancer mortalities in children. Because neural crest cells are multipotent and migratory, neuroblastoma is highly heterogenous and frequently metastatic at diagnosis, making it difficult to treat (2). Members of the receptor tyrosine kinase (RTK) family are known to regulate cell fate in neural crest and neuroblastoma cells and inappropriate signaling through RTK pathways are thought to contribute to neuroblastoma (3).

Among the downstream effectors of RTKs are Src-family kinases (SFKs), a family of non-receptor tyrosine kinases, which regulate migration, proliferation and differentiation. Upon activation of RTKs by external ligands, SFKs are recruited to the cytoplasmic tails of RTKs and phosphorylated, stabilizing them in the active form (4, 5). SFKs are further regulated by their location within the cell. Localization to lipid rafts can cluster SFKs with signaling partners. SFKs can also be endocytosed, where they can continue to signal from the surface of early and recycling endosomes, or be sequestered within the intraluminal vesicles (ILVs) of multivesicular endosomes (MVEs), carrier vesicles destined to fuse with late endosomes (6, 7, 8, 9). Once in ILVs, SFKs can be targeted to lysosomes and degraded, or released in exosomes. Exosomes are small extracellular vesicles (30-100nm in diameter) that are released when MVBs fuse with the plasma membrane. Exosomes are released by most cells in the body and carry out a number of functions. In cancer, they have been implicated in promoting metastasis and tumor-formation (10).

The scaffolding protein, PAG1, binds SFKs and controls their activity by regulating their movement within the cell and mediating their interaction with C-terminal SRC kinase (CSK), which down-regulates SFK activity by phosphorylating inhibitory residues (5). Previous studies have shown that after stimulation of SH-SY5Y neuroblastoma cells with RTK ligands, PAG1 is enriched in cell fractions containing the two SFKs, FYN and LYN (11). To investigate the role of PAG1 in SFK trafficking, a knock-down of PAG1 was attempted by transfecting SH-SY5Y cells with CRISPR/Cas9 plasmids targeting the PAG1 gene. Gene-sequencing of mutated SH-SY5Y

cells revealed a homozygous frameshift mutation, resulting in an early stop-codon, down-stream of the transmembrane region. Mass spectrometry and Western blotting analysis of mutants revealed expression of a truncated PAG1 protein, transcribed from a down-stream start codon. Since these cells express PAG1 which lacks the transmembrane domain, they are referred to as PAG1™- cells.

Here, I show that PAG1™- cells exhibit increased proliferation in comparison to wild-type SH-SY5Y (WT) cells. Flow cytometry experiments have shown that PAG1™- cells contain higher levels of active, phospho-SFKs (pSFKs). Based on this, we hypothesized that increased proliferation may be the result of hyper-active SFKs. To test this, I performed cell growth assays measuring the effects of SFK inhibition by PP2 treatment on proliferation in WT cells and PAG1™- cells. Surprisingly, I found that PAG1™- mutation actually decreased sensitivity to PP2. This led us to ask whether SFK activity is altered by differences in intracellular trafficking in PAG1™- cells. Because previous data sets had indicated that FYN and LYN change location in response to RTK signaling (11), we have focused our experiments on these two SFKs. While fractionation experiments with PAG1™- and WT cells did not indicate significant differences between location of FYN or LYN in endosomes, protease protection experiments suggested that pSFKs are targeted to MVBs in PAG1™- cells. Since cargo in MVBs is primarily targeted either to the lysosome or released in exosomes, we hypothesized that PAG1™- would alter the incorporation of SFKs into exosomes. To test this, I isolated exosomes from both WT and PAG1™- cells to compare SFK content.

Methods

MTT assays:

PAG1™- and WT cells were seeded at 50,000 cells/well for 2-day experiments and 15,000 cells/well for 3-day experiments in 96-well plates in 10%FBS RPMI 1640 medium. Day 0 wells were seeded from the same cell suspension as Day 2 or Day 3 wells, onto separate plates. At least six wells were seeded for each condition, and at least six blank wells were included on each plate to measure for background absorbance. One day after seeding, Day 0 measurements were taken. Seeding medium was replaced with 100μL 0.45mg/ml Thiazolyl Blue Tetrazolium Bromide (MTT) and left for four hours at 37°C to react with metabolizing cells. After 4 hours, 100μL of sodium dodecyl sulfate (SDS) in hydrochloric acid (pH=2) was added to each well to quench the reaction and dissolve the solid formazan product. After the formazan crystals had dissolved, absorbance at 570nm was measured by a VersaMax plate reader (Molecular Devices). For treatment wells, seeding medium was replaced with either PP2 (200nM, 500nM and 5μM) medium or vehicle control medium containing DMSO (ranging from 0.006% to 0.015% DMSO). Cells were left for either 2 or 3 days in treatment, after which MTT reactions were carried out,

using the same procedure as for Day 0 wells. Previously conducted experiments showed that a linear relationship exists between cell number and absorbance at 570nm for absorbance values below 1.5 (data not shown). All absorbance readings for these experiments were less than 1.0 and were assumed to be directly proportional to the number of cells. The median blank absorbance was subtracted from all other absorbance readings from the same plate individually, and all subsequent calculations used background-corrected absorbance readings.

Growth rate calculations:

Growth rate refers to the number of doublings per day, as given by the formula:

$$R = [log_2(A_t/A_0)]/t$$

where R is the calculated growth rate, A_0 and A_t are the absorbance measurements before and after treatment, respectively, and t is the number of days for which cells were grown in PP2 or control medium. Growth rate was calculated for each Day 2 or Day3 well individually using the median A_0 value. A small number of wells generated negative growth rates, and were excluded from the data. If a set of replicate wells had more than two missing values, the whole set of data was also excluded. GRIs were calculated as described by Hafner et al., by the formula:

$$GRI = 2^{R'/R} - 1$$

where *R'* is the growth rate of cells under the test condition, and R is the control growth rate. In the case of PAG1-GRIs, R and *R'* are the growth rates of WT and PAG1™- cells respectively. For PP2-GRIs R is the growth rate of cells in vehicle-control medium, and *R'* the growth rate of cells in PP2 medium. GRIs were calculated as the outer product, using each replicate *R'* value in combination with each replicate R value. These calculations were carried out for five experiments individually. The resulting GRIs were pooled, and the second and third quartiles were used for analysis by plotting and in Welch's t-tests. One-sample t-tests were also calculated for PP2-GRIs, to determine the statistical significance of growth rate inhibition (as indicated by deviation from 1). Calculations and graphs were done using the statistical programming language, *R*.

Exosome isolation and analysis:

WT and PAG1™- cells were grown to between 90 and100% confluency, and media was replaced with serum-free DMEM, 24 hours prior to media collection. Conditioned media was centrifuged at 2,000 x *g* for 20 minutes, then 5,000 x *g* for 60 minutes to remove larger fragments. Exosomes were then pelleted by ultracentrifugation of the supernatant at 194,000 x *g* for 90 minutes. Pellets were then dissolved in 7M Urea buffer containing SDS and heated at 55º for 15 minutes. Samples were separated by SDS-PAGE. Western blots were stained with antibodies specific for FYN, LYN, pSRC and CD9 and imaged in a Fujifilm LAS-3000.

Intensities of each SFK signal was divided by the intensity of CD9 from the same exosome sample to get an SFK/CD9 ratio for each cell type. The SFK/CD9 ratio for each cell type was then divided by the SFK/CD9 ratio in WT exosomes, as described by the formula:

$$(\frac{PAG1^{TM-}SFK}{PAG1^{TM-}CD9})/(\frac{WTSFK}{WTCD9})$$

Results

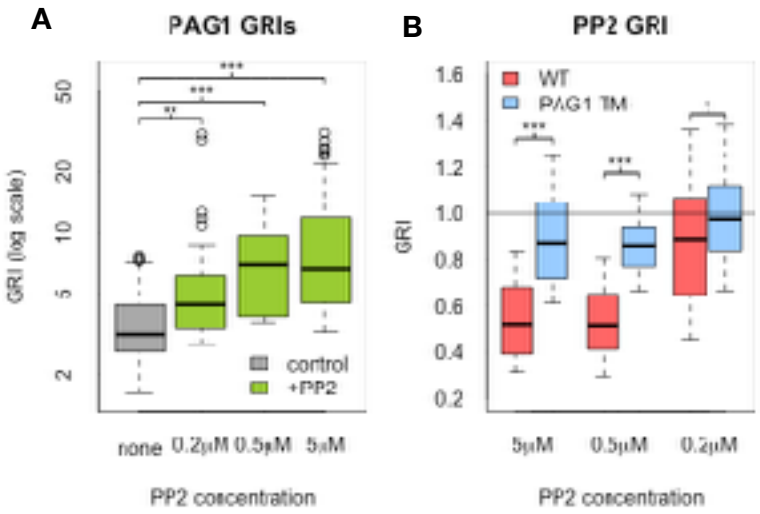

Figure 1: GRIs reveal increased growth rate in PAG1^{TM-} cells and decreased sensitivity to PP2. Data was collected from five experiments. Boxplots show the interquartile range of PAG1-GRIs (**A**) and PP2-GRIs (**B**) for each concentration of PP2. *P<0.05, **P<0.005, ***P<0.0005. Student's t test was also calculated for pooled growth rates of WT vs. PAG1^{TM-} cells. All P-values were less than 0.05.

PAG1^{TM-} increases proliferation and decreases sensitivity to SFK inhibitor

To determine the effects of PAG1^{TM-} mutation on proliferation, MTT assays were used to measure the growth rate of WT and PAG1^{TM-} cells over 2 or 3 day growth periods. Effects on growth rate were interpreted by calculating the growth rate index (GRI), a normalized ratio which is robust against factors such as seeding density or culture volume, which are known to alter other growth rate metrics (12). Data were pooled from five replicate experiments. Due to high variability and the presence of outliers in the data, I restricted my analysis to the interquartile ranges of GRIs. PAG1-GRIs are the normalized ratio of PAG1^{TM-} growth rates to WT growth rates. PAG1-GRIs were significantly greater than 1 under control conditions (Fig. 1A, left) indicating that PAG1^{TM-} increased proliferation.

Since PAG1^{TM-} cells had been shown to contain higher levels of pSFKs, we wanted to determine whether SFK activity was responsible for the increased proliferation in PAG1^{TM-} cells. To test this, I determined the growth rates of cells grown in the presence of PP2, an SFK inhibitor. PP2 is a tyrosine kinase inhibitor which is specific for SFKs at low concentrations (IC_{50} for SFKs ranges from approximately 5nM to 100nM (13, 14)), but can have off-target effects on other tyrosine kinases including the EGF receptor (IC_{50} ~480nM) (14). PP2 was added to culture

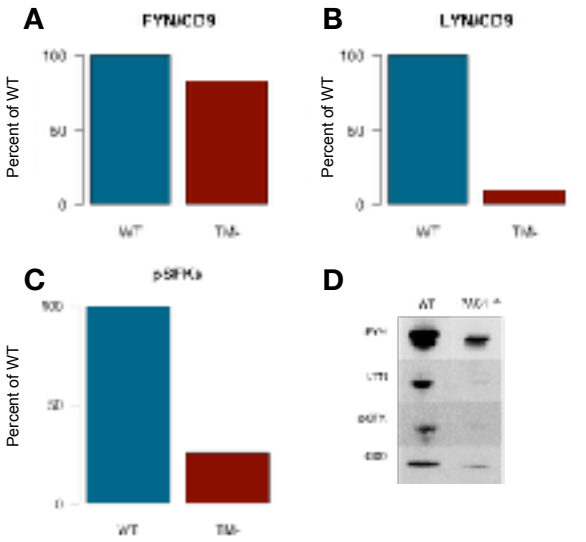

Figure 2: PAG1™- decreases LYN and pSFK in exosomes. Exosomes were isolated from WT and PAG1™- cells and probed for FYN, LYN, pSFK and CD9. To determine the relative amount of SFKs expressed in exosomes, the FYN(**A**), LYN (**B**) and pSFK (**C**) signal was divided by the CD9 signal for each sample. The resulting SFK to CD9 ratio was then divided by the SFK to CD9 ratio for WT cells to get a percentage of the WT ratio. (**D**) shows Western blot images.

media at concentrations of 0.2μM, 0.5μM and 5μM. PP2-GRIs were calculated to compare proliferation during PP2 treatment to proliferation in control media. As expected PP2-GRIs were generally lower than 1 for both WT and PAG1™- cells, indicating an inhibitory effect of PP2 on proliferation. Surprisingly, PP2-GRIs of PAG1™- cells were much closer to 1 than PP2-GRIs of WT cells for all concentrations of PP2, indicating that PAG1™- cells were less sensitive to SFK inhibition by PP2 than WT cells (Fig. 1B). At the lowest concentration of PP2, PP2-GRIs for PAG1™- cells were not significantly different from 1 (based on a Welch's t-test), indicating growth rates of PAG1™- cells were not affected by PP2 at 0.2μM. WT cells however, did display decreased proliferation, with PP2-GRIs significantly lower than 1 (P=1.3x10^{-3}).

PP2 treatment also increased PAG1-GRIs compared to untreated cells. Increasing concentration of PP2 exacerbated this difference, as PAG1-GRIs are significantly higher in cells treated with 5μM PP2 than in those treated with either 0.2μM or 0.5μM PP2 (P=1.7x10^{-3} and P=2.2x10^{-2}, respectively).

PAG1™- decreases incorporation of LYN and pSFKs in exosomes

To determine whether PAG1™- alters incorporation of SFKs into exosomes, I isolated exosomes from WT and PAG1™- cells via ultracentrifugation. Protein contents of exosome samples were separated and analyzed on a Western blot. In addition to FYN, LYN and pSFKs, I probed samples for the exosomal marker, CD9, also known as Tetraspanin-29 (15) (Fig. 2D). Because CD9 is a general exosome marker, involved in clustering of cargo into ILVs, I assumed the intensity of CD9 to be proportional to the amount of exosomes in each sample, and the ratio of SFKs to CD9 to be proportional to the density of SFKs in exosomes. Because different antibodies have different binding characteristics, direct comparison between different probes is not meaningful. Instead, I focused on the differences in SFK densities between WT and PAG1™- cells. Following this logic, each SFK signal was divided by the CD9 signal for each sample, to obtain SFK/CD9 ratios. To normalize between SFKs, each SFK/CD9 ratio was then divided by

the corresponding WT SFK/CD9 ratio, and shown as a percentage (Fig. 2A-C). I found that PAG1™- decreased the density of LYN in exosomes (Fig. 2B) but had a negligible effect on FYN (Fig. 2A). Surprisingly, PAG1™- exosomes also contained lower levels of pSFKs than WT exosomes (Fig. 2C).

Discussion

SFKs are known to be important in controlling cell fate, yet the precise roles of different SFKs are not well-characterized. SFKs act within dense and overlapping signaling networks, in which phosphorylation, as well as intracellular location regulate their activity. Localization of SFKs to lipid rafts is known to increase SFK activities by bringing them into proximity with signaling partners (5). Signaling kinases which are targeted to endosomes, but remain on the cytosolic surface of early endosomes, can continue to transduce signals by interacting with cytosolic proteins (7). On the other hand, movement of signaling proteins into MVEs can sequester them from target proteins, and thereby down-regulate their activity (9). From MVEs, cargo is typically moved into lysosomes to be degraded, or secreted in exosomes (10). PAG1 binds SFKs to facilitate their interaction with regulatory proteins (5). We believe that PAG1 also directs their movement within signaling compartments.

Here, I have shown that cells expressing PAG1™- proliferate faster than WT cells (Fig. 1A). Because previous experiments have shown that PAG1™- cells contain higher levels of pSFKs (unpublished data), we hypothesized that hyper-activation of SFKs in PAG1™- cells led to increased proliferation. However, proliferation assays with the SFK-inhibitor PP2, showed that PAG1™- cells were less sensitive to PP2 than WT cells (Fig. 1). This may have to do with the particular SFKs which are hyper-activated in PAG1™- cells. While SRC is known to drive proliferation (11), other SFKs may have suppressive effects on proliferation. FYN and LYN are both driven out of lipid rafts and into lysosomes in response to stimulation of pro-pluripotency RTKs, suggesting that they may promote a more differentiated, and less proliferative phenotype for neuroblastoma cells (11).

It is also important to note that increased phosphorylation of SFKs does not necessarily imply increased signaling ability. Decreased sensitivity to PP2 in PAG1™- cells, could also be related to the location of SFKs within PAG1™- cells. Protease protection experiments have indicated that FYN, LYN and pSFKs are all abundantly trafficked to MVEs in PAG1™- cells, whereas only LYN is trafficked to MVEs in WT cells (Lauren Foltz, unpublished observations). Previous studies have shown that SH-SY5Ys release exosomes containing LYN and, to a lesser extent, FYN (9, 16). I have shown that exosomes released by PAG1™-expressing SH-SY5Y cells contained lower levels of LYN and pSFKs (Fig. 2A,C). The density of FYN in PAG1™- exosomes was similar to that in WT exosomes (Fig. 2B). Since more FYN is targeted to MVEs

in PAG1™- cells than in WT cells, this would still imply that a decreased fraction of the total FYN in PAG1™- MVEs is incorporated into exosomes. This may suggest that SFKs in the MVEs of PAG1™- cells are mainly targeted to lysosomes for degradation, rather than being released in exosomes, although this would need to be tested directly.

How MVEs are targeted to exosomes, as opposed to lysosomes is not well understood. PAG1 may be required to escort SFKs, or simply to direct SFKs towards MVEs which are destined to release exosomes. Further studies into how cargo in MVEs is targeted to the correct destination may help elucidate the role of PAG1 and SFKs in regulating cell fate of neuroblastoma cells.

References:

1. Bronner, M.E., and N.M. LeDouarin. 2012. Development and evolution of the neural crest: An overview. *Dev. Biol*. 366(1):2–9.
2. Davidoff, A.M. 2012. Neuroblastoma. *Semin. Pediatr. Surg.* 21(1):2–14.
3. Mei, Y., Z. Wang, L. Zhang, Y. Zhang, X. Li, H. Liu, J. Ye, and H. You. 2012. Regulation of neuroblastoma differentiation by forkhead transcription factors FOXO1/3/4 through the receptor tyrosine kinase PDGFRA. *Proc. Natl. Acad. Sci.* 109(13):4898–4903.
4. Lemmon, M.A., and J. Schlessinger. 2010. Cell signaling by receptor tyrosine kinases. *Cell.* 141(7): 1117–34.
5. Ingley, E. 2008. Src family kinases: Regulation of their activities, levels and identification of new pathways. *Biochim. Biophys. Acta - Proteins Proteomics*. 1784(1):56–65.
6. de Diesbach, P., T. Medts, S. Carpentier, L. D'Auria, P. Van Der Smissen, A. Platek, M. Mettlen, A. Caplanusi, M.-F. van den Hove, D. Tyteca, and P.J. Courtoy. 2008. Differential subcellular membrane recruitment of Src may specify its downstream signaling. *Exp. Cell Res.* 314(7):1465–1479.
7. Pereira, D.B., and M. V Chao. 2007. The Tyrosine Kinase Fyn Determines the Localization of TrkB Receptors in Lipid Rafts. *J Neurosci*. 27(18):4859 – 4869
8. Sorkin, A., and M. von Zastrow. 2009. Endocytosis and signalling: intertwining molecular networks. *Nat. Rev. Mol. Cell Biol.* 10(9):609–22.
9. Taelman, V.F., R. Dobrowolski, J.-L. Plouhinec, L.C. Fuentealba, P.P. Vorwald, I. Gumper, D.D. Sabatini, and E.M. De Robertis. 2010. Wnt Signaling Requires Sequestration of Glycogen Synthase Kinase 3 inside Multivesicular Endosomes. *Cell*. 143(7):1136–1148.
10. Keerthikumar, S., L. Gangoda, M. Liem, P. Fonseka, I. Atukorala, C. Ozcitti, A. Mechler, C.G. Adda, C.-S. Ang, and S. Mathivanan. 2015. Proteogenomic analysis reveals exosomes are more oncogenic than ectosomes. *Oncotarget*. 6(17):15375–96.

11. Palacios-Moreno, J., L. Foltz, A. Guo, M.P. Stokes, E.D. Kuehn, L. George, M. Comb, and M.L. Grimes. 2015. Neuroblastoma Tyrosine Kinase Signaling Networks Involve FYN and LYN in Endosomes and Lipid Rafts. *PLOS Comput. Biol.* 11(4):e1004130.

12. Hafner, M., M. Niepel, M. Chung, and P.K. Sorger. 2016. Growth rate inhibition metrics correct for confounders in measuring sensitivity to cancer drugs. Nat. Methods. 13(6):521–527.

13. Hanke, J.H., J.P. Gardner, R.L. Dow, P.S. Changelian, W.H. Brissette, E.J. Weringer, B.A. Pollok, and P.A. Connelly. 1996. Discovery of a novel, potent, and Src family-selective tyrosine kinase inhibitor. Study of Lck- and FynT-dependent T cell activation. *J. Biol. Chem*. 271(2):695–701.

14. Bain, J., L. Plater, M. Elliott, N. Shpiro, C.J. Hastie, H. Mclauchlan, I. Klevernic, J.S.C. Arthur, D.R. Alessi, and P. Cohen. 2007. The selectivity of protein kinase inhibitors: a further update. *Biochem. J*. 408(3):297–315.

15. Jeppesen, D.K., A.M. Fenix, J.L. Franklin, J.N. Higginbotham, Q. Zhang, L.J. Zimmerman, D.C. Liebler, J. Ping, Q. Liu, R. Evans, W.H. Fissell, J.G. Patton, L.H. Rome, D.T. Burnette, and R.J. Coffey. 2019. Reassessment of Exosome Composition. *Cell.* 177(2):428–445.e18.

16. Colletti, M., A. Petretto, A. Galardi, V. Di Paolo, L. Tomao, C. Lavarello, E. Inglese, M. Bruschi, A.A. Lopez, L. Pascucci, B. Geoerger, H. Peinado, F. Locatelli, and A. Di Giannatale. 2017. Proteomic Analysis of Neuroblastoma-Derived Exosomes: New Insights into a Metastatic Signature. *Proteomics*. 17(23–24):1600430.